Electronic Supplementary Information (ESI)

Thermocatalytic cleavage of C–C and C–O bonds in model compounds and kraft lignin by $NiMoS_2$/C nanocatalyst

Swathi Mukundan,[a,b] Luqman Atanda,[a,c] and Jorge Beltramini*[c,d]

[a.] *Nanomaterials center- AIBN and School of chemical engineering, The University of Queensland, Brisbane, QLD-4072, Australia.*

[b.] *Department of Applied Chemistry, Cochin University of Science and Technology, Kochi, Kerala- 682022, India.*

[c.] *Centre for Tropical Crops and Biocommodities, Queensland University of Technology, Brisbane, QLD- 4000, Australia*

[d.] *IROAST, Department of Chemistry, Faculty of Advanced Science and Technology, Kumamoto University, Kumamoto 860-8555, Japan.*

Kraft Lignin Conversion and product Analysis Calculations

Initially, 1.5 g of alkali lignin was stirred with methanol for 30 min at room temperature. The methanol–soluble low molecular weight products were removed. The methanol insoluble lignin was retrieved, dried and used for the depolymerization reaction.

Weight of lignin after methanol washing= 1.3 g

Catalyst used = 10 wt%= 0.13 g

After reaction, the product was filtered. The total solid collected was 0.43 g

Solid contains catalyst+ coke+ unreacted lignin

The lignin used in this study was reported to be soluble in 1 M NaOH. After washing with 20 mL of 1M NaOH, the remaining solid collected after drying was 0.28 g.

So unreacted lignin was 0.43 g- 0.28 g= 0.15 g

Coke produced was 0.28 g- 0.13 g= 0.15 g

% conversion= weight of lignin in feed- (weight of unreacted lignin)/ weight of lignin in feed = 1.3-(0.15)/1.3= 88.5 % conversion

% unreacted lignin= 100- 88.5= 11.5 % unreacted lignin

% yield of char= weight of char/weight of reacted lignin*100= 0.15/1.15*100= 13.05 % char

% yield of liquids= % conversion- % yield of char = 88.5-13.05=75.45% yield of liquids

Table S1 Textural properties of activated carbon, MoS_2/C, and $NiMoS_2$/C catalysts

Support/ catalyst	BET surface area (m^2g^{-1})			Pore size (nm)[b]	Pore volume (cm^3g^{-1})		
	Micro[a]	Meso	Total		Micro	Meso	Total
Carbon	705	358	1063	3.95	0.36	0.62	0.98
MoS_2/C	49	116	165	3.9	0.022	0.25	0.27
$NiMoS_2$/C	45	108	153	3.9	0.023	0.19	0.21

[a] calculated by BET t–plot micropore area [b] Pore size calculated by BJH method from desorption isotherm

Table S2 Surface and bulk elemental analysis of MoS_2/C and $NiMoS_2$/C catalysts.

Catalyst	Surface composition[a] (at. %)					Bulk composition[b] (at. %)				
	Mo	Ni	S	Ni: Mo	S: Mo	Mo	Ni	S	Ni: Mo	S: Mo
MoS_2/C	5.3	–	10.3	–	1.95:1	1.9	–	3.9	–	2.05:1
$NiMoS_2$/C	5.1	1.5	9.8	0.29:1	1.92:1	1.55	0.61	3.2	0.25:1	2.05:1

[a] Analysed by XPS, catalysts are reduced before analysis but not protected from exposure to air. [b] Analysed by ICP, catalysts are reduced before analysis but not protected from exposure to air.

Table S3 The number of methoxyl and hydroxyl units in the lignin model compounds studied

Model compound	**Methoxyl**	**Hydroxyl**
Syringol	2	1
Veratrole	2	0
Guaiacol	1	1
Phenol	0	1

Table S4. Yield of liquid products obtained from Kraft lignin depolymerisation reaction with 10 wt % $NiMoS_2$/C catalyst at 300 ˚C, 50 bar initial H_2 pressure and 3 h reaction time

Total yield of monomers= 18.98 %

Total yield of identified monomers = 12.92%

Total yield of non-identified monomers = 6.06%

S. No	**Expected Compound as per Library**	**Weight (mg)**	**Yield (%)**
1	Hexane	3.89 mg	0.4 %
2	Methyl cyclopentane	26.8 mg	2.73 %
3	Methyl tetrahydrofuran	1.6 mg	0.16 %
4	Toluene	1.25 mg	0.13 %
5	Phenol	1.9 mg	0.19 %
6	Guaiacol	3.1 mg	0.31 %
7	2-methyl phenol	2.68 mg	0.27 %
8	3-methyl phenol	66.4 mg	6.77 %
9	4– ethyl guaiacol	19.2 mg	1.96 %
Total		126.82 mg	12.92 %

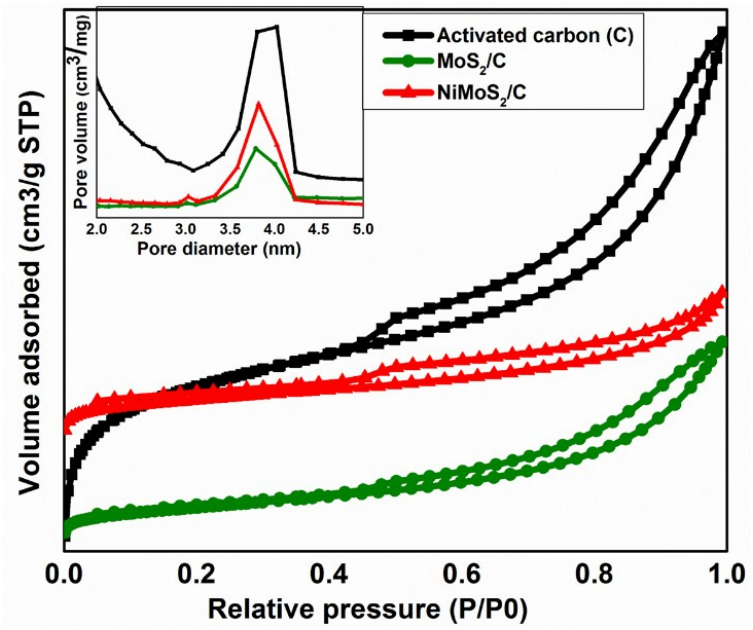

Fig. S1 Nitrogen adsorption isotherms and pore size distribution curves of activated carbon, MoS_2/C and $NiMoS_2$/C catalysts

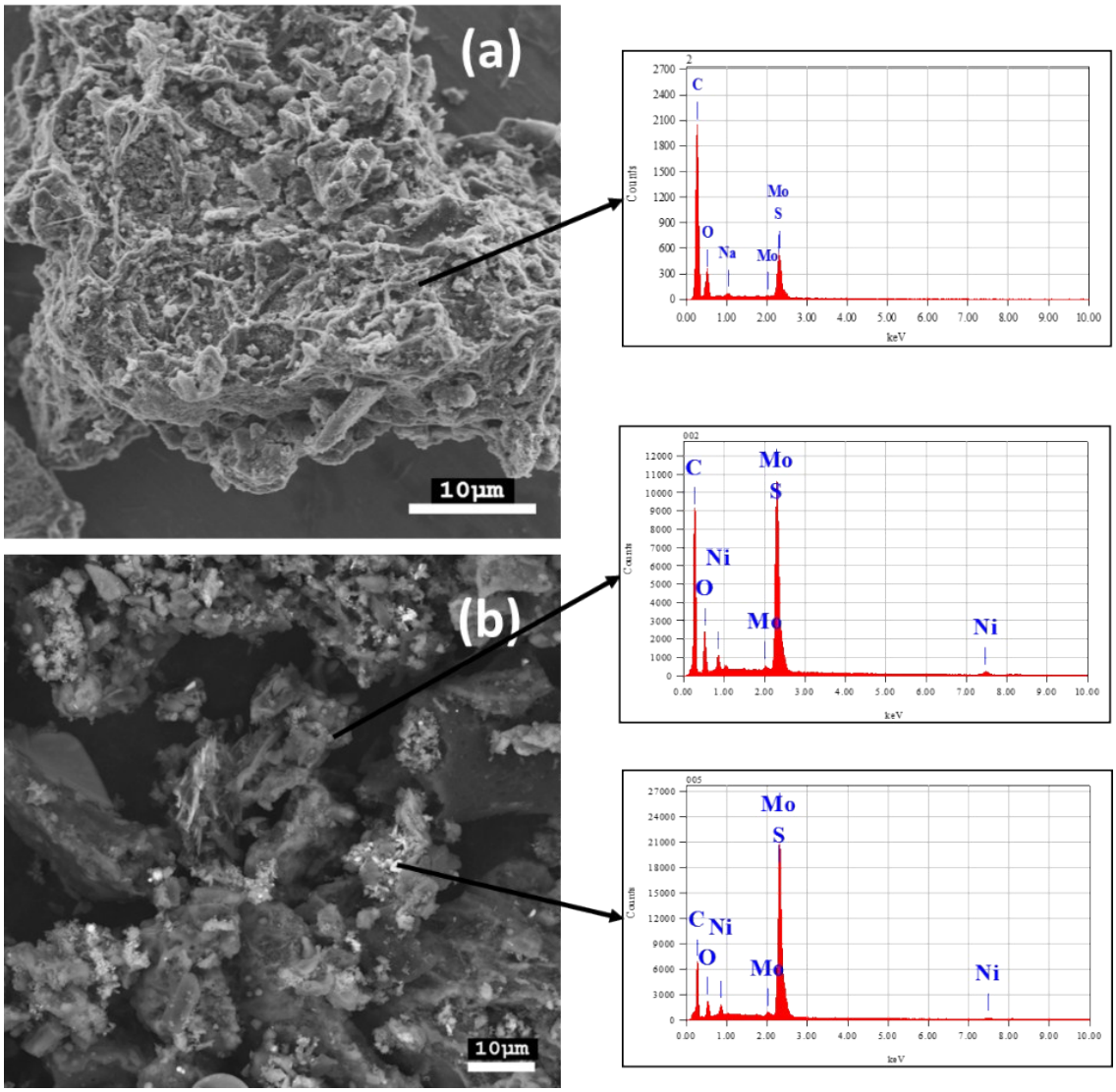

Fig. S2 FE–SEM images and their corresponding EDX spectra of (a) MoS_2/C and (b) $NiMoS_2$/C catalysts.

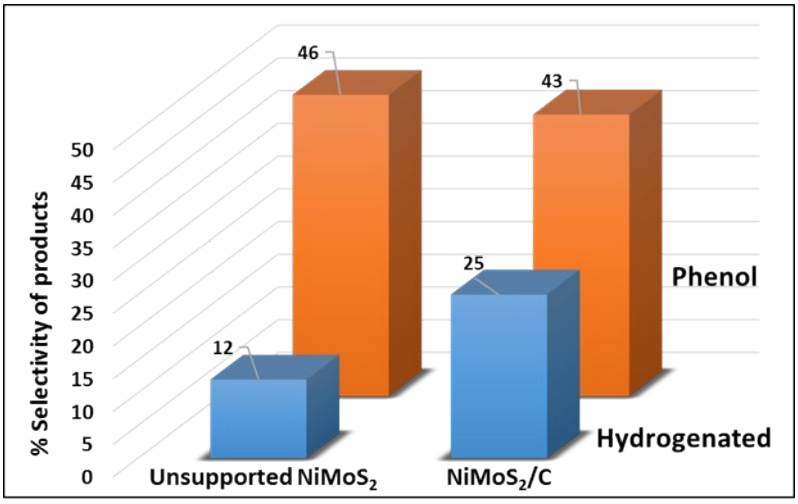

Fig. S3 Selectivity of liquid products (%) for the conversion of guaiacol by (a) unsupported $NiMoS_2$ and (b) $NiMoS_2$/C catalysts.

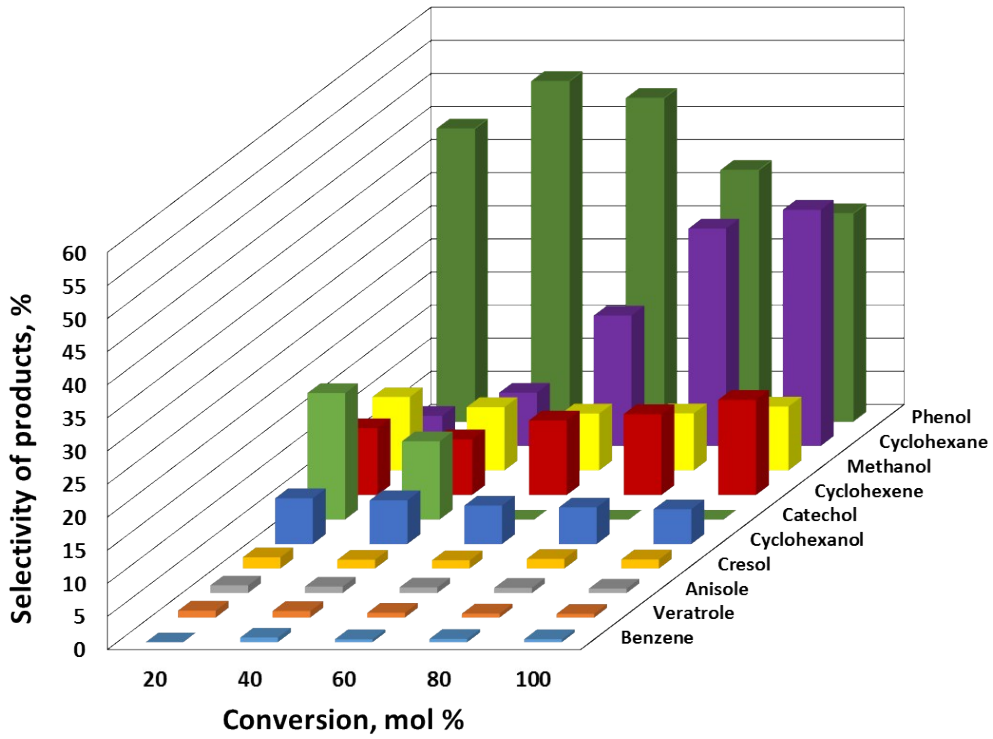

Fig. S4 Conversion, mol % of guaiacol and selectivity (%) of products in liquid phase with $NiMoS_2$/C catalyst

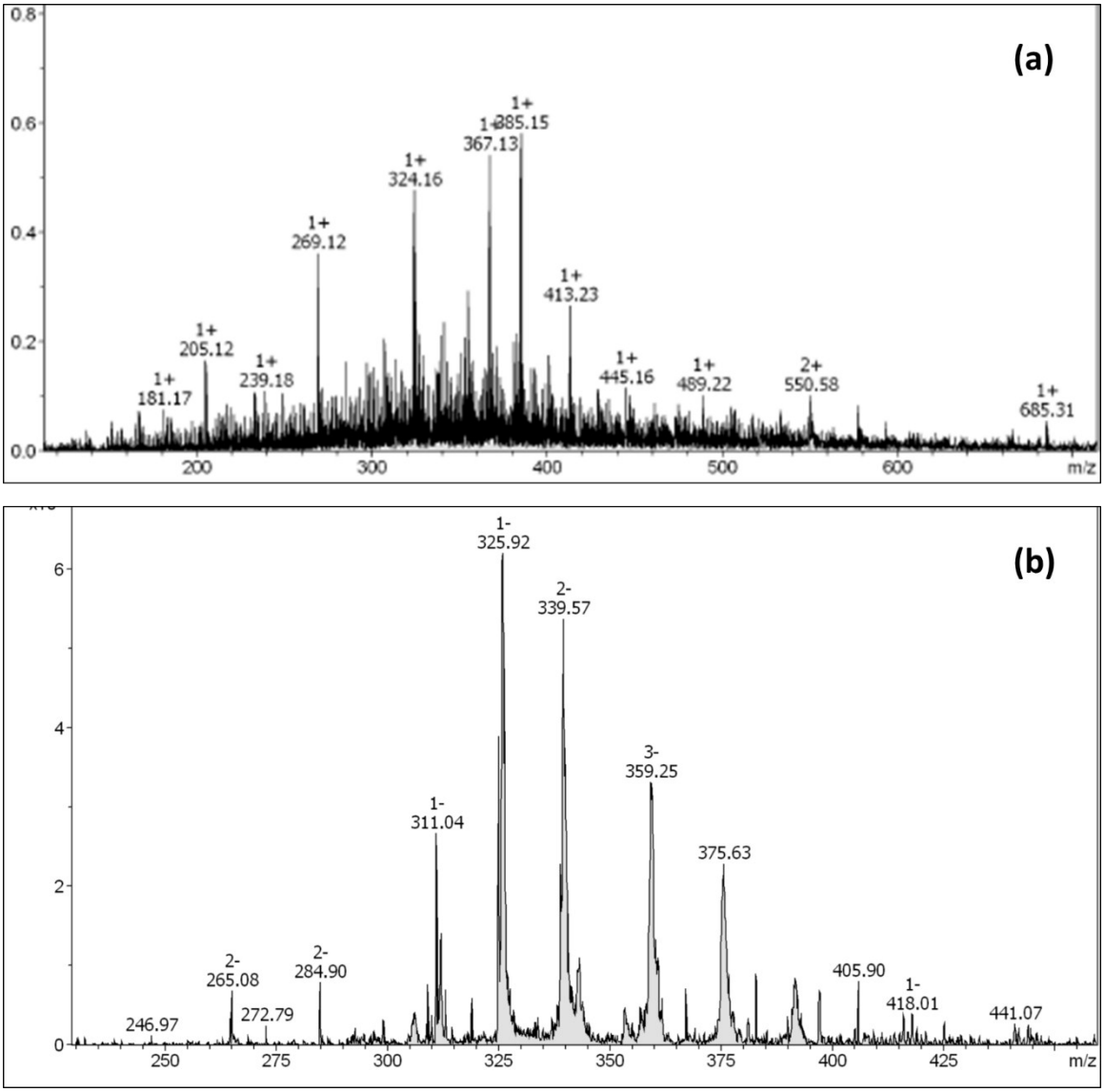

Fig. S5 Low–resolution mass spectrum of the liquid fraction obtained after 3 h of alkali lignin depolymerisation reaction (a) in positive ionisation mode (b) in negative ionisation mode.

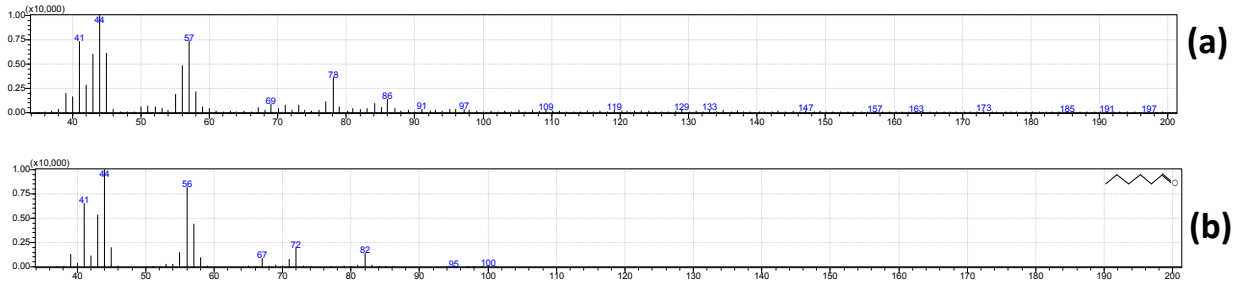

Fig. S6 Mass spectrum of: a) hexane in the reaction product b) standard hexane

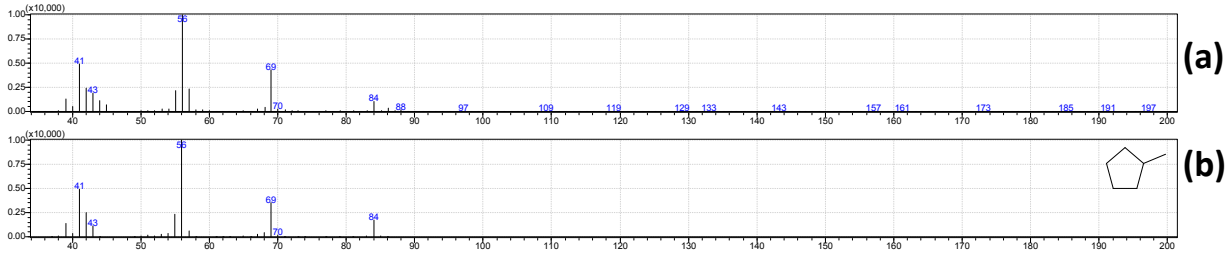

Fig. S7 Mass spectrum of: a) methyl cyclopentane in the reaction product b) standard methyl cyclopentane

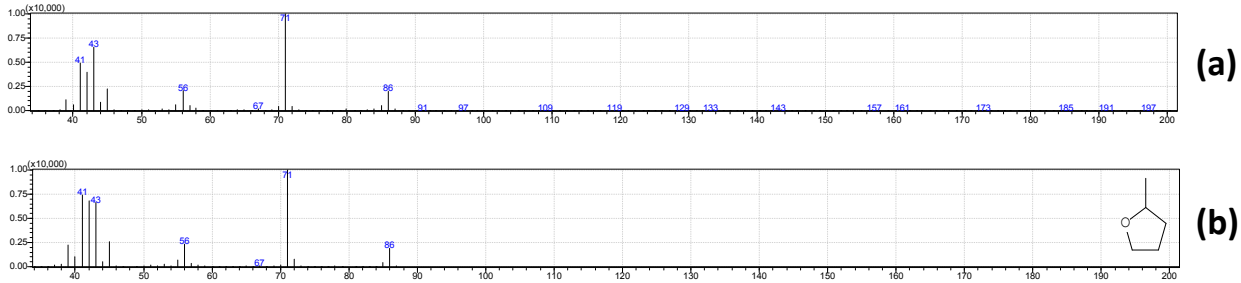

Fig. S8 Mass spectrum of: a) methyl tetrahydrofuran in the reaction product b) standard methyl tetrahydrofuran

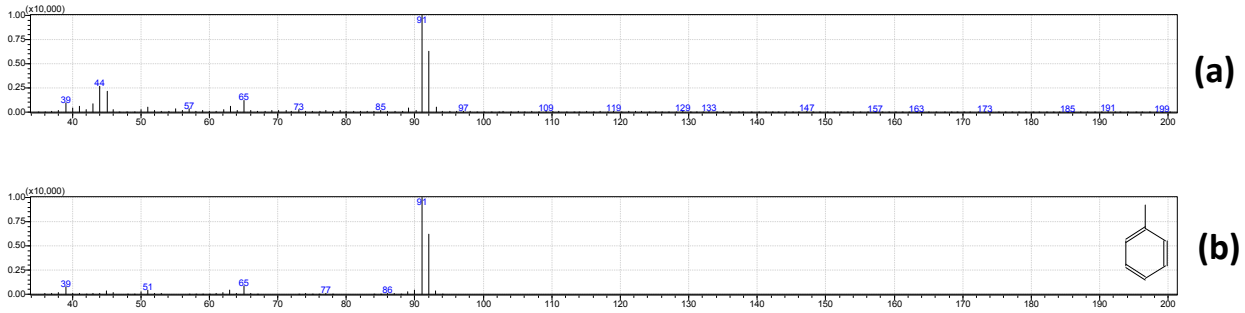

Fig. SS9 Mass spectrum of: a) toluene in the reaction product b) standard toluene

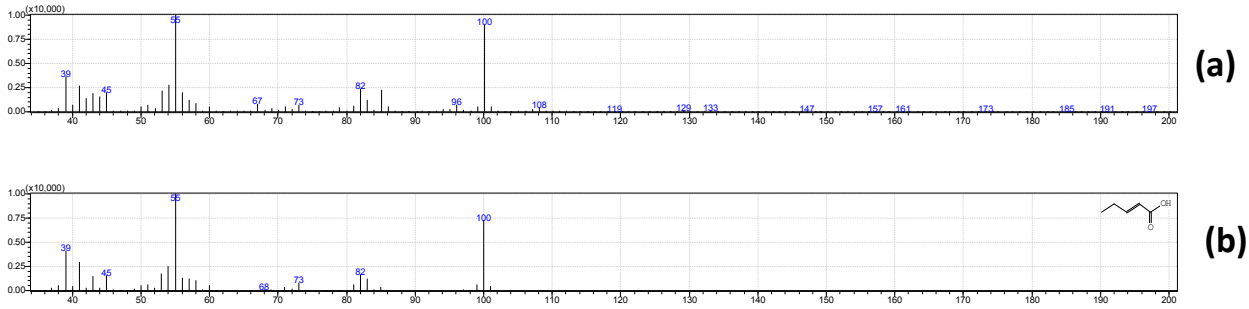

Fig. S10 Mass spectrum of: a) trans 2-pentanoic acid in the reaction product b) standard trans 2-pentanoic acid

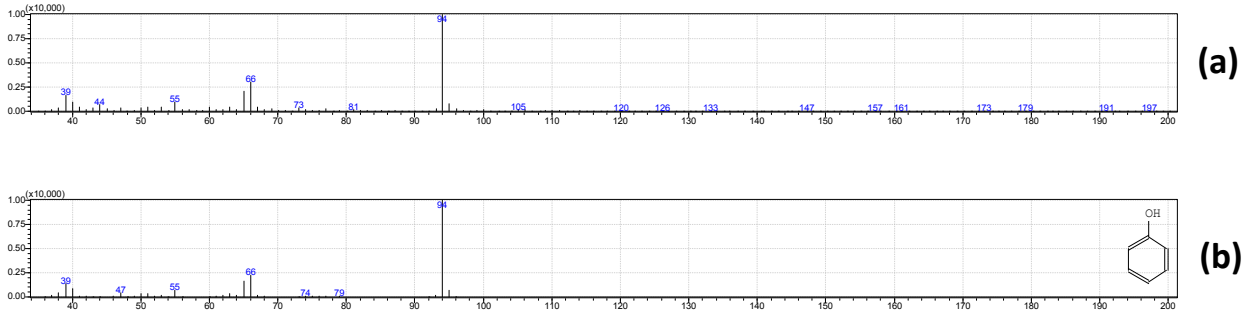

Fig. S11 Mass spectrum of a) phenol in the reaction product b) standard phenol

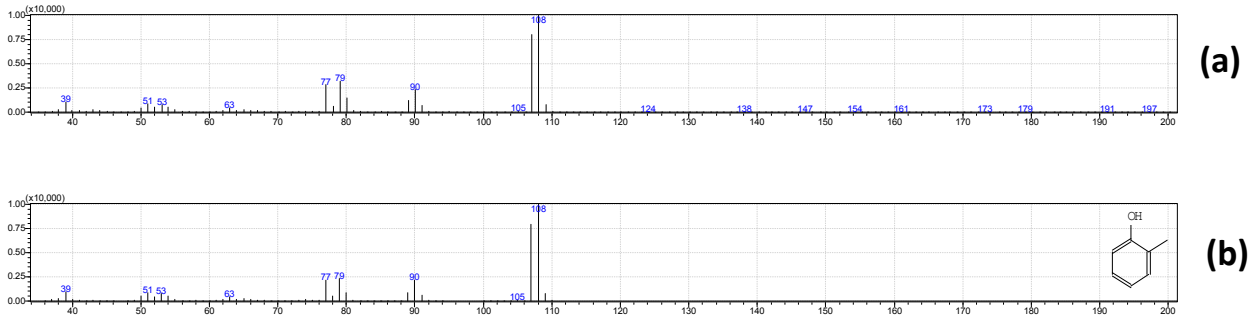

Fig. S12 Mass spectrum of a) 2-methyl phenol in the reaction product b) standard 2-methyl phenol

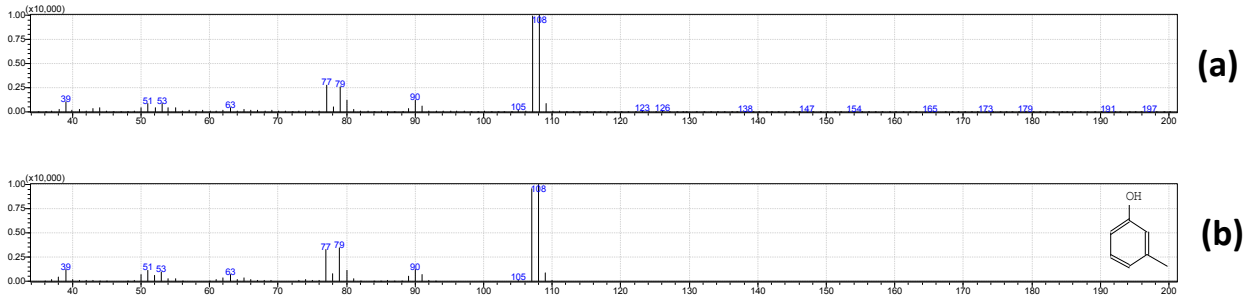

Fig. S13 Mass spectrum of a) 3-methyl phenol in the reaction product b) standard 3-methyl phenol

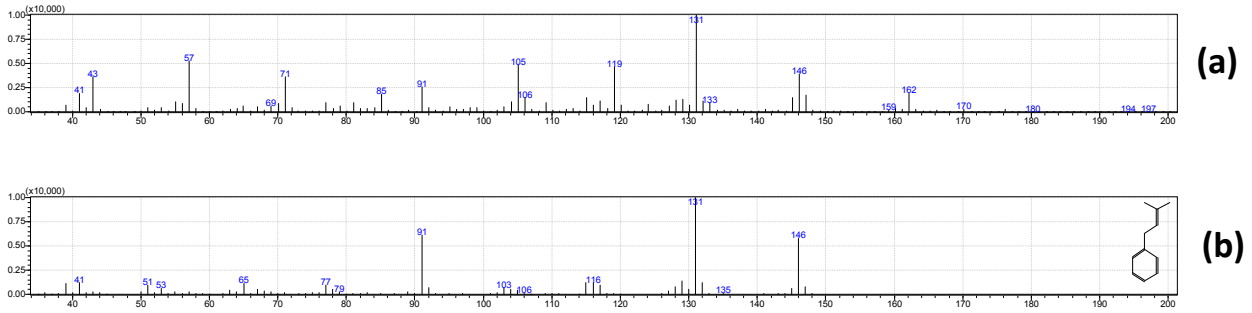

Fig. S14 Mass spectrum of a) 3-methyl-2-butenyl benzene in the reaction product b) standard 3-methyl-2-butenyl benzene

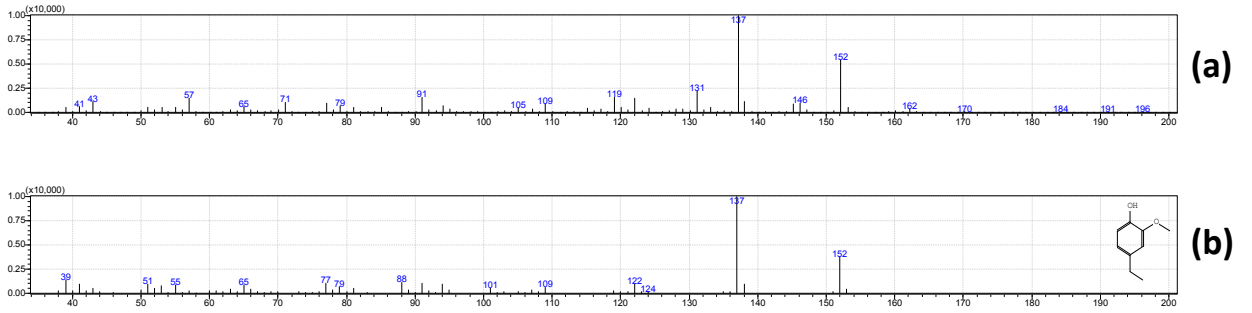

Fig. S15 Mass spectrum of a) 4-ethyl guaiacol in the reaction product b) standard 4-ethyl guaiacol

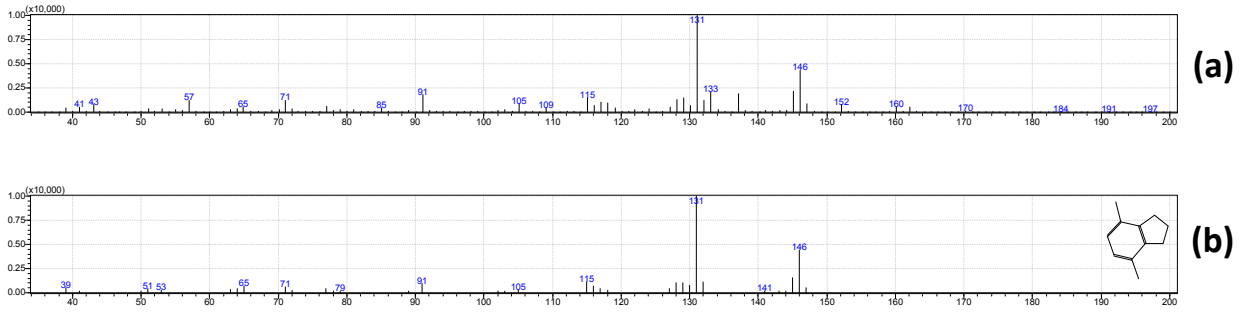

Fig. S16 Mass spectrum of a) 4,7-dimethyl-2,3-dihydro-1H-indene in the reaction product b) standard 4,7-dimethyl-2,3-dihydro-1H-indene

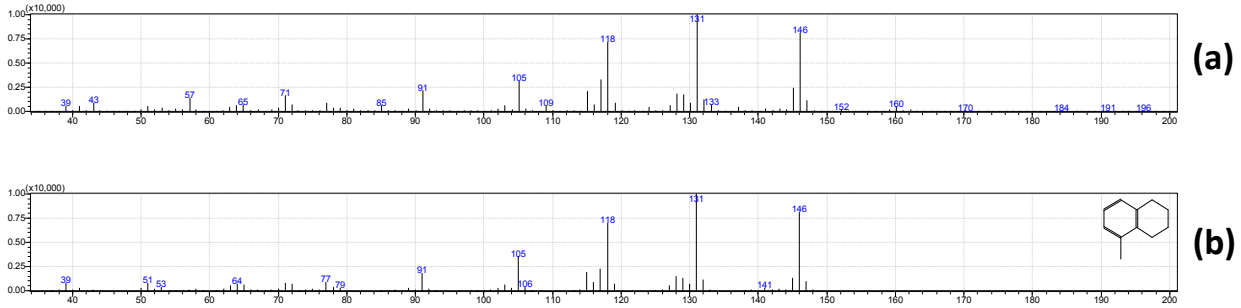

Fig. S17 Mass spectrum of a) 1,2,3,4-tetrahydro-1-methyl naphthalene in the reaction product b) standard 1,2,3,4-tetrahydro-1-methyl naphthalene

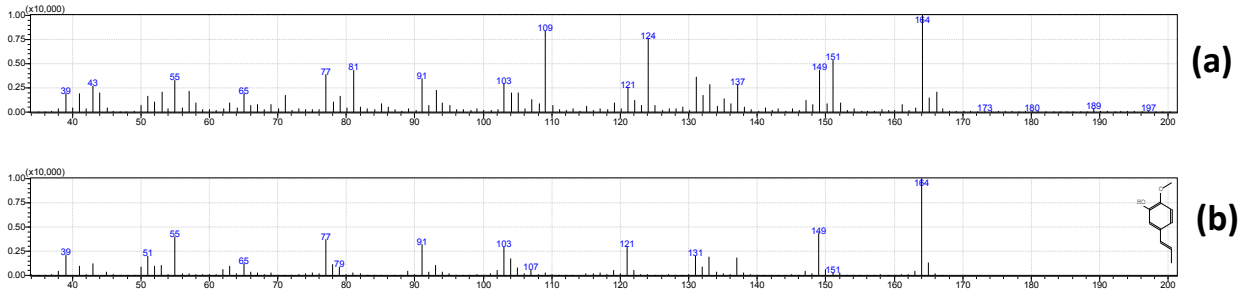

Fig. S18 Mass spectrum of a) trans m-propenyl guaiacol in the reaction product b) standard trans m-propenyl guaiacol

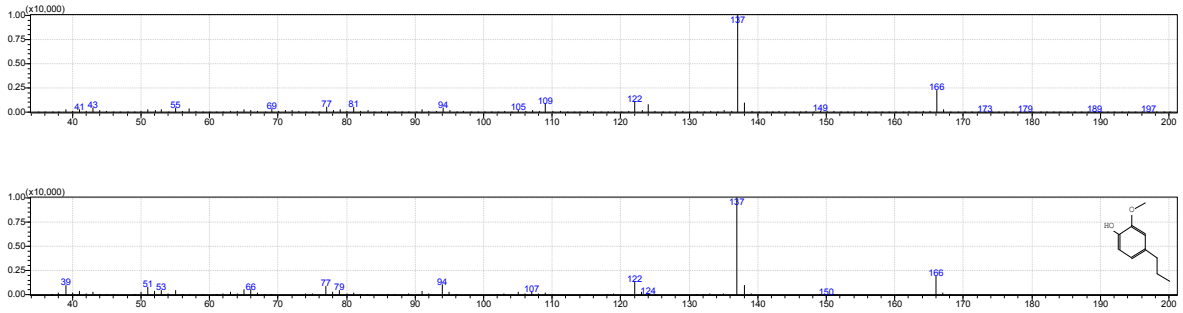

Fig. S19 Mass spectrum of a) 2-methoxy 4-propyl guaiacol in the reaction product b) standard 2-methoxy 4-propyl guaiacol

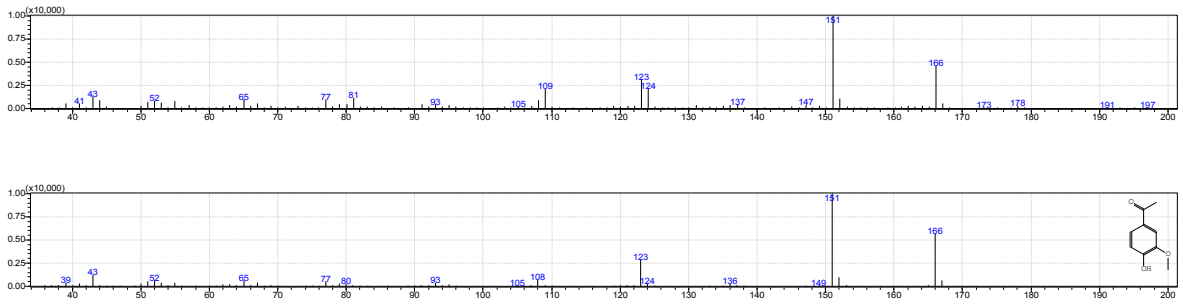

Fig. S20 Mass spectrum of a) 2-acetoguaiacone in the reaction product b) standard 2-acetoguaiacone.

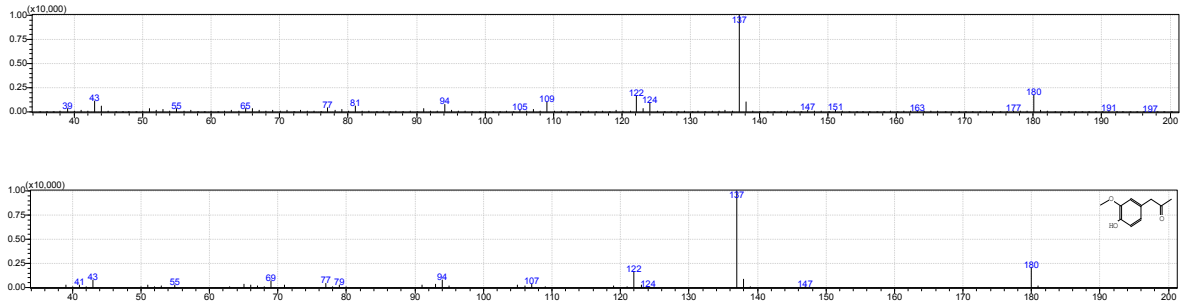

Fig. S21 Mass spectrum of a) guaiacyl acetone in the reaction product b) standard guaiacyl acetone

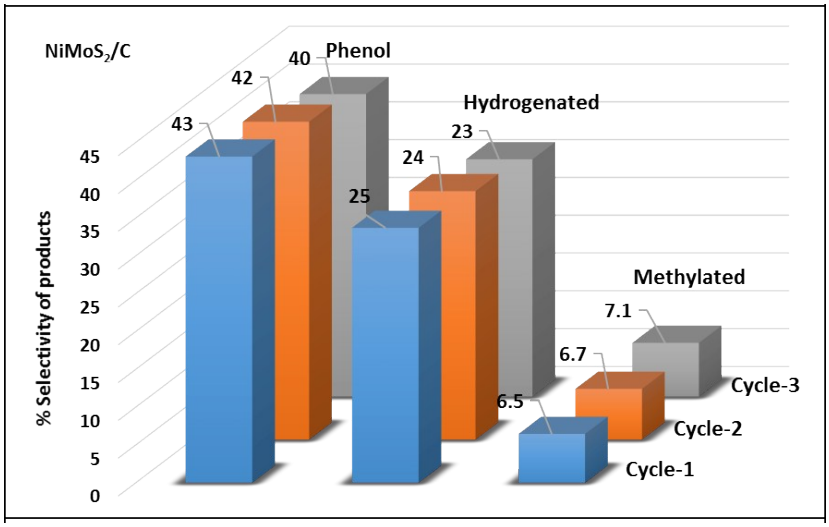

Fig. S22 Selectivity of liquid products (%) by $NiMoS_2/C$ catalysts for conversion of guaiacol after 5 h reaction.

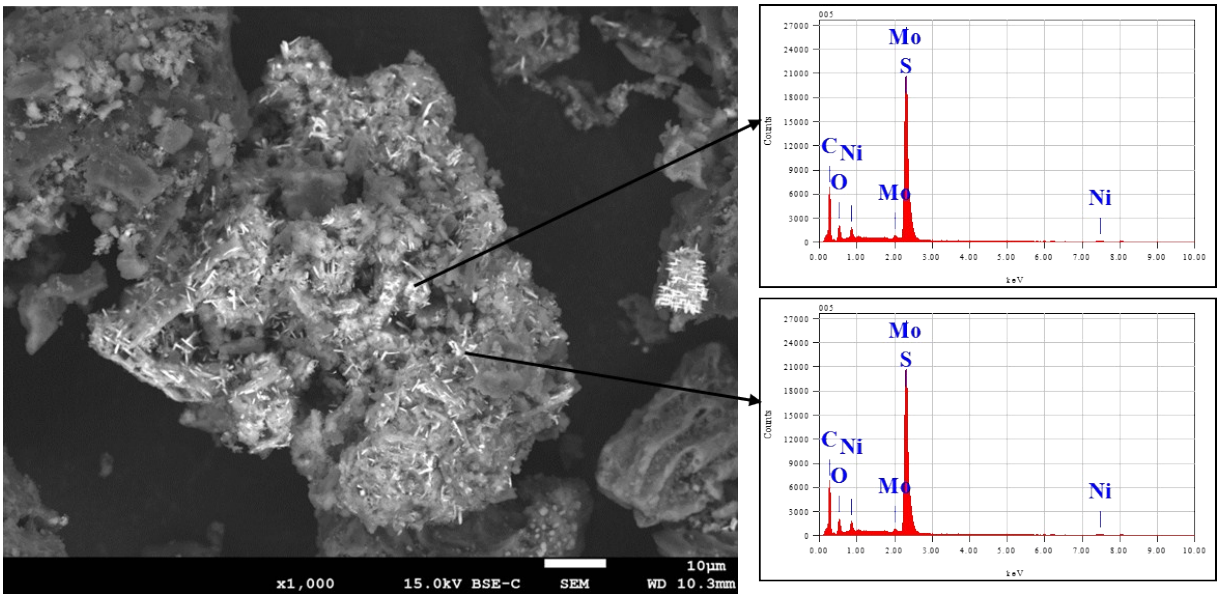

Fig. S23 FE–SEM images of $NiMoS_2$/C catalysts after cycle–3.

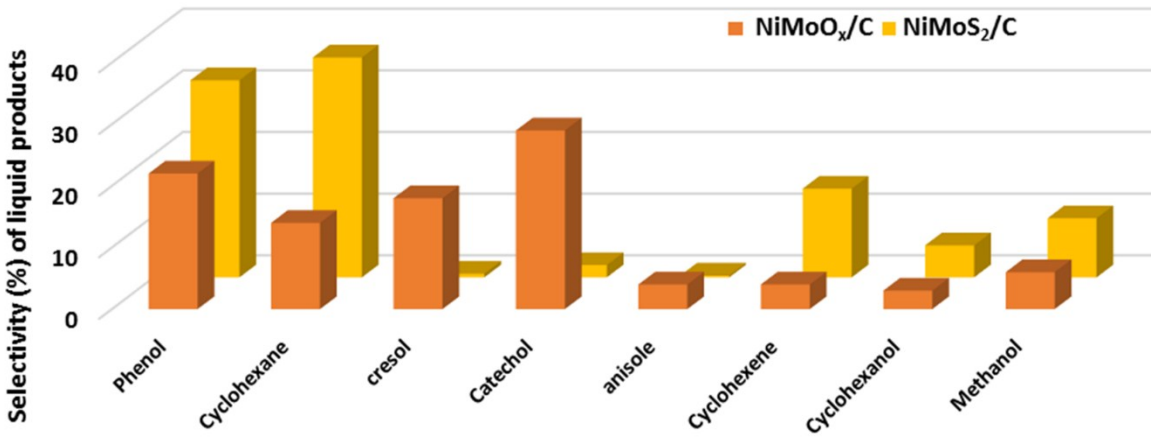

Fig. S24 Comparison of liquid product selectivities for the conversion of guaiacol with $NiMoO_x$/C and $NiMoS_2$/C catalysts at the end of 5 h.